Close-limit analysis for head-on collision of two black holes in higher dimensions: Brill-Lindquist initial data

Hirotaka Yoshino,[1,*] Tetsuya Shiromizu,[1,2,3,†] and Masaru Shibata[4,‡]

[1]*Department of Physics, Tokyo Institute of Technology, Tokyo 152-8551, Japan*
[2]*Department of Physics, The University of Tokyo, Tokyo 113-0033, Japan*
[3]*Advanced Research Institute for Science and Engineering, Waseda University, Tokyo 169-8555, Japan*
[4]*Graduate School of Arts and Sciences, University of Tokyo, Komaba, Meguro, Tokyo 153-8902, Japan*

(Received 17 August 2005; published 21 October 2005)

Motivated by the TeV-scale gravity scenarios, we study gravitational radiation in the head-on collision of two black holes in higher-dimensional spacetimes using a close-limit approximation. We prepare time-symmetric initial data sets for two black holes (the so-called Brill-Lindquist initial data) and numerically evolve the spacetime in terms of a gauge-invariant formulation for the perturbation around the higher-dimensional Schwarzschild black holes. The waveform and radiated energy of gravitational waves emitted in the head-on collision are clarified. Also, the complex frequencies of fundamental quasinormal modes of higher-dimensional Schwarzschild black holes, which have not been accurately derived so far, are determined.

DOI: 10.1103/PhysRevD.72.084020 PACS numbers: 04.70.−s, 04.30.Db, 04.50.+h, 11.25.−w

I. INTRODUCTION

Clarifying the nature of black holes in higher-dimensional spacetimes has become an important issue since the possibility of the black-hole production in accelerators was pointed out. If our space is the 3-brane in large [1] or warped [2] extra dimensions, the Planck energy could be of O(TeV) that is accessible with the planned accelerators. If the number of dimension D of our spacetime is actually larger than 4, a black hole of very small mass will be produced artificially in particle experiments and the evidence may be detected.

The possible phenomenology of the black holes which may be produced in accelerators was first discussed in [3] (see [4] for reviews). During the high-energy particle collision of a sufficiently small impact parameter in a higher-dimensional spacetime, two particles will form a distorted black hole of small mass. Subsequently, it settles down to a stationary state after emission of gravitational waves. The stationary black hole will soon be evaporated by the Hawking radiation, indicating that the quantum gravity effects will be important. The evaporation and quantum gravity effects [5,6] have been studied for yielding a plausible scenario (cf. [7] for related issues). On the other hand, the analyses for formation of the black hole and for the subsequent evolution by gravitational radiation are still in an early stage. These phases are described well in the context of general relativity [8] (see also [9]), but due to its highly nonlinear nature, the detailed process has not been well understood.

More specifically, two issues should be clarified for these phases. One is the condition (i.e., the impact parameter) for formation of a black hole and the other is the fate of the formed black hole after emission of gravitational waves, which can be used as the initial condition of the Hawking radiation phase.

Extensive effort has been made in the past five years for the first issue. The popular method is to approximate the high-energy particle of no charge or spin by the Aichelburg-Sexl shock-wave metric [10]. The merit of this approximation is that superimposing two Aichelburg-Sexl metrics, a metric of two particles moving with the speed of light can be derived for a spacetime region in which causal connection between two particles is absent. Although this solution can form a naked singularity at the collision and it is not clear what happens after the collision, it is still possible to determine the condition for the formation of an apparent horizon for a spacelike hypersurface of the known solution. Formation of the apparent horizon is a sufficient condition for formation of a black hole for which the event horizon is outside the apparent horizon. Thus, the lower bound of the impact parameter can be estimated. Such study was first done by Eardley and Giddings [11] in a four-dimensional case and it was extended to D-dimensional cases by Yoshino and Nambu [12]. Recently these studies were improved by Yoshino and Rychkov [13] by analyzing the apparent horizon in a different spacelike hypersurface from the one in [11,12].

The second issue is to clarify the final state of a black hole formed after collision of two particles, which will be a Kerr black hole in higher dimensions, perhaps those described by Myers and Perry [14]. Here, the stationary Kerr black holes of no electric charge are described by the mass and angular momentum. Namely, the goal is to derive a formula of the final mass $M_{\rm final}$ and angular momentum $J_{\rm final}$ as functions of the initial impact parameter and initial energy of two particles. For this issue, a couple of prelimi-

*Electronic address: yoshino@th.phys.titech.ac.jp
†Electronic address: shiromizu@phys.titech.ac.jp
‡Electronic address: shibata@provence.c.u-tokyo.ac.jp

nary analyses have been carried out so far (see Ref. [15] for a review).

One is the work by Yoshino and Rychkov [13], who constrained the allowed region of the mass and angular momentum by finding the apparent horizon for spacetimes of two Aichelburg-Sexl particles and subsequently employing the area theorem. However, the allowed region cannot be pinpointed with this approach, implying that the analysis of gravitational waves emitted during the collision is inevitable.

The gravitational radiation from two particles with the speed of light in a head-on collision was first computed by D'Eath and Payne [16] (summarized in [17]). They analyzed a spacetime of two Aichelburg-Sexl particles in the $D = 4$ case, paying attention only to a region far from the particles and using a perturbative theory. By this analysis, the radiation near the symmetric axis can be calculated. Assuming the axisymmetric angular pattern of the radiation, they estimated the total radiated energy $E_{\rm rad}$ as 16% of the total energy of the system.

Recently, Cardoso *et al.* [18] studied gravitational radiation in the linear perturbation theory of the higher-dimensional flat spacetime. They found again that about 16% of the total energy will be emitted in the head-on collision for $D = 4$, which is consistent with the results by D'Eath and Payne. They also found that the efficiency is highly suppressed for a larger value of D, e.g., about 0.001% for $D = 10$.

The black-hole perturbation theory has also been used recently. Cardoso *et al.* [19] computed gravitational waves from a particle of energy μ with a speed close to the light speed falling straightforwardly into a Schwarzschild black hole of mass $M \gg \mu$ for $D = 4$. Berti *et al.* [20] extend their work for $D > 4$ (see [21] for further generalizations). Extrapolating the results for $\mu \to M/2$, they found that the radiation efficiency is $\approx 13\%$ for $D = 4$ and decreases by increasing the value of D, e.g., 8% for $D = 10$.

Although these approximate studies could give an approximate value of the radiation efficiency, it is natural to consider that the error in the estimate is still a factor of 2 or more. To derive the exact numerical value, it is necessary to carry out a more strict analysis. One promising approach is to employ numerical simulation in full general relativity. In the $D = 4$ case, simulation for black-hole collision is feasible [22], producing certain scientific results. However, these works have been done for the case that the velocity of each black hole is much smaller than the speed of light. Formulation and numerical technique for black-hole collision with a very large Lorentz factor $\gamma \gg 1$ have not been developed yet.

In this paper, we adopt the so-called close-limit method for computing gravitational radiation, which was originally developed by Price and Pullin [23]. In this method, we prepare two black holes of a small separation as the initial condition. If the separation is small enough to form a common horizon, the spacetime can be well approximated by a perturbed black-hole spacetime. As a result, the gravitational radiation during the collision can be analyzed in the context of the black-hole perturbation theory. This method has been applied for two black holes initially at rest [24,25], initially approaching with linear momentum [26], and many other two-black-hole systems [27]. The robustness of this method is established by confirming that the results by this method agree with those in numerical relativity. This fact motivates us to adopt the close-limit approximation for high-velocity collision of two black holes in higher-dimensional spacetimes.

As a first step toward the series of study for more plausible cases, in this paper, we focus on head-on collision with time-symmetric initial data of two equal-mass black holes. For simplicity, we choose the Brill and Lindquist initial data [28] that describes a spacelike hypersurface in a spacetime composed of three sheets connected by two Einstein-Rosen bridges. We will show the successful numerical results and indicate that extension of the analyses with more general initial data is straightforward.

This paper is organized as follows. In the Sec. II, we introduce the Brill-Lindquist initial data and analyze the apparent horizons for $D \geq 4$. In Sec. III, we derive the close-limit form of the initial data and briefly review the master equation for the perturbation of the higher-dimensional Schwarzschild black hole [29]. We also explain our numerical methods. Numerical results are shown in Sec. IV, paying attention to the radiated energy and gravitational waveforms. Section V is devoted to a summary. In Appendix A, the gauge-invariant perturbation formalism as well as a method for preparing an initial master variable from the Brill-Lindquist initial data are presented. Appendix B describes a formula for computing the radiated energy of gravitational waves from the master variable.

II. THE BRILL-LINDQUIST INITIAL DATA

A. The Brill-Lindquist two-black-hole solution

Let (Σ, h_{ab}, K_{ab}) denote a $(D-1)$-dimensional spacelike hypersurface Σ with the metric h_{ab} and the extrinsic curvature K_{ab} in a D-dimensional spacetime. The equations of the Hamiltonian and momentum constraints are

$$ {}^{(n+1)}R - h^{ab}h^{cd}K_{ac}K_{bd} + K^2 = 0, \tag{1} $$

$$ \nabla^a(K_{ab} - h_{ab}K) = 0, \tag{2} $$

where ${}^{(n+1)}R$ is the Ricci scalar of Σ, ∇^a is the covariant derivative with respect to h_{ab}, and $n = D - 2$. Assuming the time symmetry (i.e., $K_{ab} = 0$), Eq. (2) is satisfied trivially. Assuming further the conformal flatness $h_{ab} = \Psi^{4/(n-1)}\delta_{ab}$, the Hamiltonian constraint equation is written to the Laplace equation for the conformal factor

$$\nabla_{\rm f}^2 \Psi = 0, \tag{3}$$

where $\nabla_{\rm f}^2$ is the flat-space Laplacian.

We introduce the cylindrical coordinates (ρ, z) in which the flat-space metric is given by $ds_{\rm f}^2 = dz^2 + d\rho^2 + \rho^2 d\Omega_{n-1}^2$ with the metric $d\Omega_{n-1}^2$ on the $(n-1)$-dimensional unit sphere. Among an infinite number of solutions for Eq. (3) that denote spacetimes of two black holes, we choose the following one composed of two point sources located at $z = \pm z_0$ along the z axis as

$$\Psi = 1 + \frac{1}{8}[r_h(M)]^{n-1}\left(\frac{1}{R_-^{n-1}} + \frac{1}{R_+^{n-1}}\right), \tag{4}$$

where $R_\pm \equiv \sqrt{(z \mp z_0)^2 + \rho^2}$, M is the total gravitational mass of the system, and $r_h(M)$ is the gravitational radius defined by

$$r_h(M) = \left(\frac{16\pi G M}{n\Omega_n}\right)^{1/(n-1)}. \tag{5}$$

Here, $\Omega_n = 2\pi^{(n+1)/2}/\Gamma((n+1)/2)$ is the n-dimensional area of a unit sphere. Hereafter, we adopt $r_h(M)$ as the unit of the length. The solution (4) provides the system of three sheets connected by two Einstein-Rosen bridges. $r_\pm = 0$ and $r \to \infty$ correspond to spatial infinities of each sheet as found by Brill and Lindquist [28] for $D = 4$.

B. Analysis for apparent horizon

The close-limit approximation holds for the system sufficiently close to a stationary one-black-hole spacetime. Thus, this method can be applied only for the case that a common apparent horizon surrounding two black holes is present. Because of this reason, it is necessary to clarify the range of z_0 for which a common apparent horizon exists. Also, by obtaining the area of the common apparent horizon, we can estimate the lower bound of the final mass as well as the upper bound of the energy radiated away by gravitational waves, using the area theorem of black holes.

The common apparent horizon is determined by a numerical method developed by Yoshino and Nambu [30]. Since the system is axisymmetric, it is easily determined by a simple shooting method. The shape of the common apparent horizon changes from a sphere at $z_0 = 0$ to a spheroid for $z_0 > 0$, increasing the ellipticity. At a critical value, $z_0^{(\rm crit)}$, it disappears. The values of $z_0^{(\rm crit)}$ are summarized in Table I.

In the presence of the common apparent horizon, the mass of the apparent horizon is defined by

TABLE I. The critical values of $z_0^{(\rm crit)}$ for formation of a common apparent horizon for $4 \le D \le 11$.

D	4	5	6	7	8	9	10	11
$z_0^{(\rm crit)}/r_h(M)$	0.192	0.393	0.510	0.586	0.641	0.683	0.715	0.742

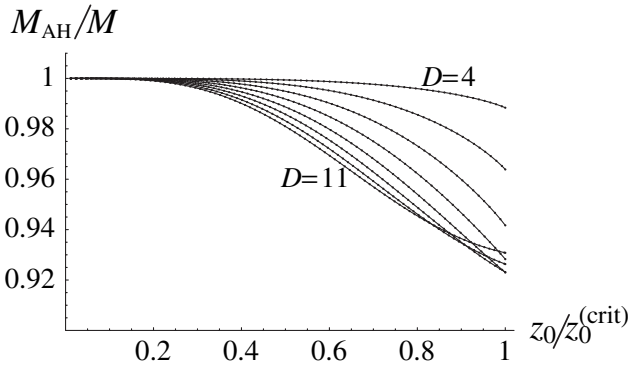

FIG. 1. The relation between $z_0/z_0^{(\rm crit)}$ and the trapped energy $M_{\rm AH}/M$ at the initial state for $D = 4$–11. The plot range of the vertical axis is $0.9 \le M_{\rm AH}/M \le 1$.

$$M_{\rm AH} = \frac{n\Omega_n}{16\pi G}\left(\frac{A_{\rm AH}}{\Omega_n}\right)^{(n-1)/n}, \tag{6}$$

where $A_{\rm AH}$ denotes the n-dimensional area of the apparent horizon. In the Brill-Lindquist initial data, $M_{\rm AH}$ coincides with the Hawking quasilocal mass [31] evaluated on the horizon and indicates the trapped energy at the initial state. $M_{\rm AH}$ provides us with the lower bound of the final mass $M_{\rm final} = M - E_{\rm rad}$ where $E_{\rm rad}$ is the radiated energy of gravitational waves. Equivalently $M - M_{\rm AH}$ gives the upper bound of $E_{\rm rad}$. Figure 1 shows the relation between $z_0/z_0^{(\rm crit)}$ and $M_{\rm AH}/M$. In the $D = 4$ case, about 99% of the total energy is trapped inside the apparent horizon at the initial state. On the other hand, the trapped energy $M_{\rm AH}/M$ becomes smaller for larger values of D.

III. THE CLOSE-LIMIT ANALYSIS

A. The close-limit of the Brill-Lindquist initial data

In this paper, the spacetime of two black holes is evolved using the close-limit approximation, in which the evolution of the field variables are carried out by a gauge-invariant perturbation technique. For this analysis, it is necessary to derive an initial condition for the linear theory in the Schwarzschild background. To do so, the Brill-Lindquist metric is rewritten to

$$ds^2 = \Psi^{4/(n-1)}[dR^2 + R^2(d\theta^2 + \sin^2\theta d\Omega_{n-1}^2)], \tag{7}$$

$$\Psi = 1 + \frac{1}{4R^{n-1}} + \frac{1}{4R^{n-1}}\sum_{l=2,4,\ldots}\left(\frac{z_0}{R}\right)^l C_l^{[(n-1)/2]}(\cos\theta), \tag{8}$$

where $R = \sqrt{z^2 + \rho^2}$, $\theta = \tan^{-1}(\rho/z)$, and $C_l^{[\lambda]}$ denotes the Gegenbauer polynomials which are defined by the generating function

$$(1 - 2xt + t^2)^{-\lambda} = \sum_{l=0}^{\infty} C_l^{[\lambda]}(x) t^l. \tag{9}$$

Here, we assume $z_0 \ll r_h(M) = 1$. If $z_0 = 0$, the metric provides the space component of the Schwarzschild metric in the isotropic coordinate.

We introduce a new coordinate r through the ordinary relation between the Schwarzschild coordinate r and the isotropic coordinate R:

$$r = R\Psi_0^{2/(n-1)}, \qquad \Psi_0 = 1 + 1/4R^{n-1}, \tag{10}$$

or equivalently

$$R = \left[\left(r^{(n-1)/2} + \sqrt{r^{n-1} - 1}\right)/2\right]^{2/(n-1)}. \tag{11}$$

Then the metric becomes

$$ds^2 = \left(\frac{\Psi}{\Psi_0}\right)^{4/(n-1)}\left[\frac{dr^2}{1 - 1/r^{n-1}} + r^2(d\theta^2 + \sin^2\theta d\Omega_{n-1}^2)\right], \tag{12}$$

$$\frac{\Psi}{\Psi_0} = 1 + \frac{1/4R^{n-1}}{1 + 1/4R^{n-1}} \sum_{l=2,4,\ldots} \left(\frac{z_0}{R}\right)^l C_l^{[(n-1)/2]}(\cos\theta). \tag{13}$$

Here, the metric in the square brackets of Eq. (12) denotes the space part of the Schwarzschild metric. The difference of Ψ/Ψ_0 from unity is of $O(\epsilon^2)$ where $\epsilon \equiv z_0/R$. Since the region of $r \geq 1$ corresponds to $R \geq R_h \equiv 4^{-1/(n-1)}$, the system can be regarded as the Schwarzschild black hole plus its perturbation for a sufficiently small value of z_0 (or ϵ).

The first-order perturbation includes the mode $l = 2, 4, \ldots$ whose order is $O(\epsilon^l)$. We only consider the leading $O(\epsilon^2)$ correction which is the $l = 2$ mode. Then we find the prefactor $(\Psi/\Psi_0)^{4/(n-1)}$ of Eq. (12) becomes

$$\left(\frac{\Psi}{\Psi_0}\right)^{4/(n-1)} \simeq 1 + \frac{1/(n-1)R^{n-1}}{1 + 1/4R^{n-1}}\left(\frac{z_0}{R}\right)^2 C_2^{[(n-1)/2]}(\cos\theta). \tag{14}$$

This provides the major parts of the initial data for the linear perturbation theory in the close-limit approximation.

B. Master equations and initial master variables

In order to analyze the time evolution of the perturbation, we use a gauge-invariant formulation of the higher-dimensional Schwarzschild perturbation [29]. The master equation for the three types of perturbation variables, i.e., the scalar, vector, and tensor variables, was derived in Ref. [29]. Since the Brill-Lindquist initial data is axisymmetric with no rotation, we only need to evolve one master variable of the scalar mode.

In the scalar-mode perturbation, the master variable Φ that is related to the gauge-invariant quantities obeys the master equation

$$\frac{\partial^2\Phi}{\partial t^2} - \frac{\partial^2\Phi}{\partial r_*^2} + V_S\Phi = 0, \tag{15}$$

where

$$V_S(r) = \frac{f(r)Q(r)}{16r^2H^2(r)}, \tag{16}$$

$$f(r) = 1 - x, \qquad H(r) = m + (1/2)n(n+1)x, \tag{17}$$

$$m = k^2 - n, \qquad k^2 = l(l+n-1), \qquad x = 1/r^{n-1}, \tag{18}$$

$$Q(r) = n^4(n+1)^2x^3 + n(n+1)[4(2n^2 - 3n + 4)m + n(n-2)(n-4)(n+1)]x^2 - 12n[(n-4)m + n(n+1)(n-2)]mx + 16m^3 + 4n(n+2)m^2. \tag{19}$$

r_* denotes the tortoise coordinate defined by

$$r_* = \int dr/f. \tag{20}$$

More explicitly,

$$r_* = r - \frac{2}{n-1}\sum_{m=1}^{n/2-1} \sin\frac{2m\pi}{n-1}\left[\arctan\left(-\cot\frac{2m\pi}{n-1} + r\csc\frac{2m\pi}{n-1}\right) - \pi/2\right] + \frac{1}{n-1}\left[\log(r-1) + \sum_{m=1}^{n/2-1}\cos\frac{2m\pi}{n-1}\log\left(1 + r^2 - 2r\cos\frac{2m\pi}{n-1}\right)\right], \tag{21}$$

for even n and

$$r_* = r - \frac{2}{n-1}\sum_{m=1}^{(n-3)/2} \sin\frac{2m\pi}{n-1}\left[\arctan\left(-\cot\frac{2m\pi}{n-1} + r\csc\frac{2m\pi}{n-1}\right) - \pi/2\right] + \frac{1}{n-1}\left[\log\left(\frac{r-1}{r+1}\right) + \sum_{m=1}^{(n-3)/2}\cos\frac{2m\pi}{n-1}\log\left(1 + r^2 - 2r\cos\frac{2m\pi}{n-1}\right)\right], \tag{22}$$

for odd n.

The initial condition for the master variable Φ in gauge-invariant perturbation theory is calculated from the metric (12) and (14) numerically (see Appendix A for details). The initial values of Φ/z_0^2 for $D = 4$, 6, 8, and 10 are shown in Fig. 2. Φ/z_0^2 asymptotes to a nonzero value for

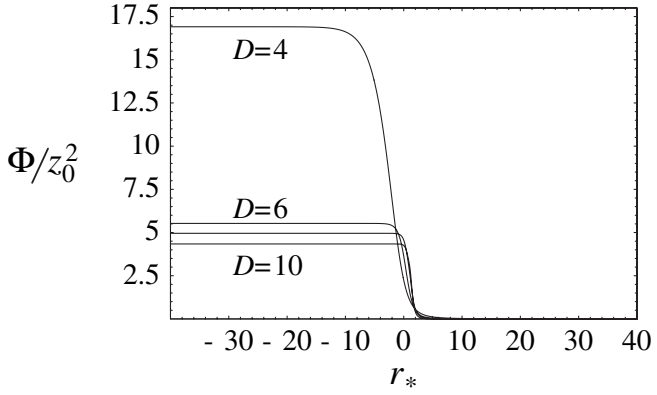

FIG. 2. The initial condition for the master variable Φ/z_0^2 as a function of r_*. The cases $D = 4$, 6, 8, and 10 are shown.

$r_* \to -\infty$ and to zero for $r_* \to \infty$. It rapidly changes around $r_* \sim 0$.

C. Numerical methods and numerical error

In the numerical computation for Eq. (15), we used the Lax-Wendroff scheme which is second-order accurate in time and space. To validate our code, the following convergence test was carried out: We evolved the Gaussian wave packet using the initial condition as $h(0, r_*) = \exp(-r_*^2/100)$ with various grid resolution. Denoting the grid spacings of r_* and t by dx and dt, respectively, there are four free parameters in our numerical code: dx, $\lambda \equiv dt/dx$, and the locations of the inner and outer boundaries $r_*^{(\mathrm{in})}$ and $r_*^{(\mathrm{out})}$. First we computed the fiducial solution $\hat{h}_N \equiv \Phi/z_0^2$ (N denotes the step size of the t direction) at $r_* = 100$ for $0 \le t \le 250$ in the $D = 4$ case, choosing $dx = 10^{-3}$, $\lambda = 0.2$, $r_*^{(\mathrm{in})} = -200$, and $r_*^{(\mathrm{out})} = 200$. Then, we repeated the computation choosing the larger values of dx while fixing the other parameters, and estimated the error by

$$\mathrm{Err} = \frac{\sum_N |h_N - \hat{h}_N|}{\sum_N |\hat{h}_N|} \tag{23}$$

for each value of dx. Figure 3 shows the relation between $\log_{10} dx$ and $\log_{10}\mathrm{Err}$. All points are located on a straight line of which slope is two. This illustrates the second-order accuracy of our code.

Then we analyzed the time evolution of the Brill-Lindquist initial data by solving the master variable Φ/z_0^2 starting with the initial values shown in Fig. 2 for $4 \le D \le 11$. We used $dx = 0.01$ for $D = 4$–7 and $dx = 0.005$ for $D = 8$–11. For the larger values of D, we choose the smaller grid spacing since the error increases with increasing D. We chose the other parameters to be $\lambda = 0.2$, $r_*^{(\mathrm{out})} = 1000$, and $r_*^{(\mathrm{in})} = -200$. Comparing the results with those computed in poorer resolutions, we found that the numerical error is within 0.02% for all values of D.

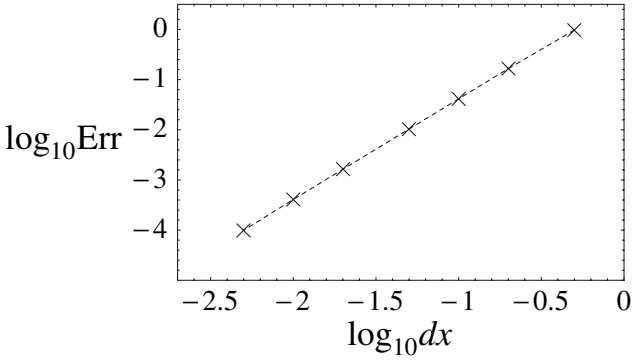

FIG. 3. The relation between the grid spacing dx of r_* and the numerical error. Our code shows the second-order convergence.

IV. NUMERICAL RESULTS

A. Waveform and radiated energy

Figure 4 shows the behavior of Φ/z_0^2 for $D = 4$–11 observed at $r_* = 100$. The quasinormal mode ringing is seen for all values of D. The power-law tail is also computed well for $D = 4$ and odd D. The reason that the tail cannot be seen for even values of $D \ge 6$ is that the tail decays more rapidly than that of odd values of D, as clarified in [32].

The total radiated energy E_{rad} is calculated by

$$\frac{E_{\mathrm{rad}}}{M} = \sum_l \frac{k^2(n-1)(k^2-n)}{2n^2\Omega_n} \int \dot{\Phi}^2 dt, \tag{24}$$

(see Appendix B for a sketch of the derivation). Since Φ is proportional to z_0^2 for the $l = 2$ mode, E_{rad} is written as

$$E_{\mathrm{rad}}/M \simeq \hat{E}_2 (z_0)^4. \tag{25}$$

Table II shows the values of $\hat{E}_2$. In the $D = 4$ case, $\hat{E}_2$ has already been obtained by Abrahams and Price [24] as $\hat{E}_2 = 0.0251$. This agrees well with our numerical result.

To compare the radiation efficiency E_{rad}/M among the different values of D, one has to specify the values of z_0. In Table II, we summarize the values at the critical values $z_0 = z_0^{(\mathrm{crit})}$ for formation of the common apparent horizon. It is found that $E_{\mathrm{rad}}(z_0^{(\mathrm{crit})})$ increases by increasing the value of D. However we also should mention that the higher-order correction might be large for $z_0 = z_0^{(\mathrm{crit})}$. As we can see from Eq. (14), the characteristic value of the first-order perturbation is $(\Psi/\Psi_0)^{4/(n-1)} - 1$, which becomes maximal at the pole on the horizon. Such a maximal value is quite large, e.g., ~ 1 for $D = 4$ and ~ 6 for $D = 10$. Although the close-limit method gives a fairly good ap-

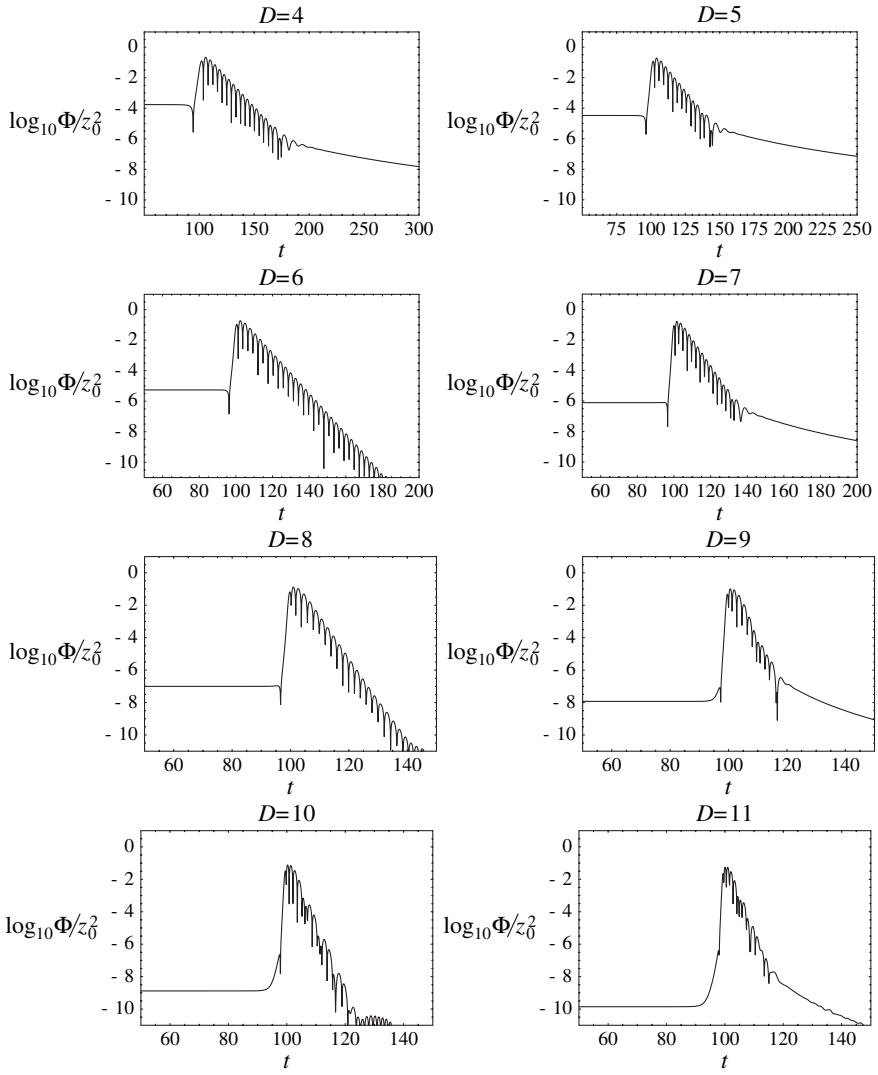

FIG. 4. Time evolution of the master variable Φ/z_0^2 observed at $r_* = 100$.

TABLE II. The values of $\hat{E}_2 \equiv E_{\rm rad}/z_0^4$ and $E_{\rm rad}$ at $z = z_0^{\rm (crit)}$ for $D = 4$–11.

D	4	5	6	7	8	9	10	11
$\hat{E}_2$	0.0252	0.0245	0.0290	0.0288	0.0258	0.0224	0.0195	0.0172
$E_{\rm rad}(z_0^{\rm (crit)})$ (%)	0.0034	0.059	0.20	0.34	0.44	0.49	0.51	0.52

proximation beyond the regime of the perturbation in the four-dimensional case [23], further investigations such as the second-order analysis or the full numerical simulation are necessary to clarify this point in higher-dimensional cases.

Figure 5 shows the energy spectrum of gravitational waves. The value of ω at the peak becomes larger as the value of D increases. This reflects the fact that the real part of the fundamental quasinormal mode frequency increases with D (see Sec. IV C for the quasinormal mode frequencies).

The angular dependence of the radiated energy is given by

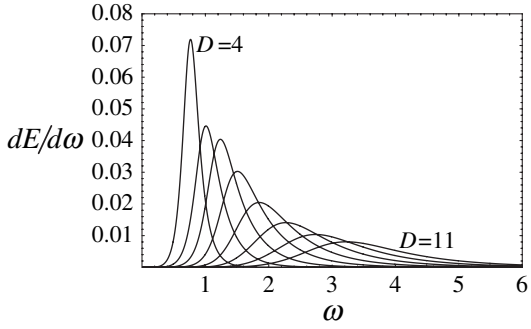

FIG. 5. The energy spectrum of gravitational waves. The unit of the vertical axis is Mz_0^4. The location of the peak shifts to the right-hand side as the value of D increases.

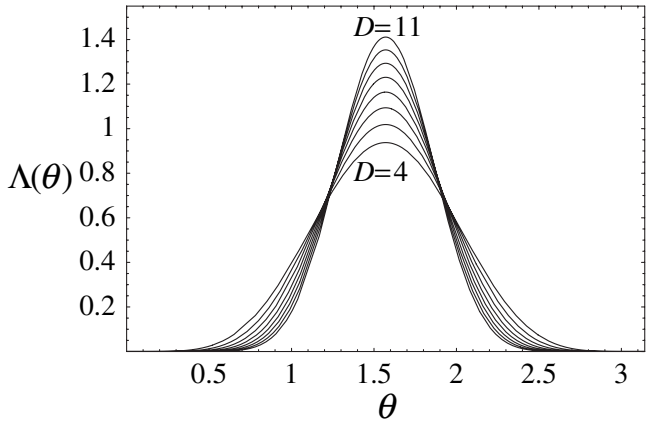

FIG. 6. The angular dependence $\Lambda(\theta)$ of the radiated energy. There is a peak at $\theta = \pi/2$ and $\Lambda(\pi/2)$ becomes larger as D increases.

$$\frac{1}{E}\frac{dE}{d\theta} := \Lambda(\theta) = \frac{\Gamma((n+5)/2)}{\sqrt{\pi}\Gamma(2+n/2)}\sin^{n+3}\theta \qquad (26)$$

(see Appendix B for a derivation). Figure 6 shows the behavior of the function $\Lambda(\theta)$ for $D = 4, \ldots, 11$. Gravitational waves are mainly emitted around the equatorial plane and this tendency is enhanced for larger D. This reflects the fact that there are more directions transverse to the symmetry axis for larger values of D.

B. Relation between $E_{\rm rad}$ and $M_{\rm AH}$

As already mentioned, $M - M_{\rm AH}$ provides the upper bound of $E_{\rm rad}$. Hence the ratio of $E_{\rm rad}$ to $M - M_{\rm AH}$

TABLE III. The values of α_D evaluated at $z_0 \ll 1$ for $D = 4, \ldots, 11$.

D	4	5	6	7	8	9	10	11
α_D	0.0034	0.016	0.024	0.024	0.021	0.017	0.014	0.011

$$\alpha_D \equiv \frac{E_{\rm rad}}{M - M_{\rm AH}} \qquad (27)$$

should be smaller than unity and it provides one consistency check of our calculation. For small value of z_0, both $E_{\rm rad}$ and $M - M_{\rm AH}$ are proportional to z_0^4, and α_D take nonzero values. The values of α_D are summarized in Table III and then we confirm that α_D is less than unity. The values of α_D in higher dimensions are larger compared to α_4 for four dimensions. The relation between $M - M_{\rm AH}$ and $E_{\rm rad}$ for $0 \le z_0 \le z_0^{\rm (crit)}$ is also depicted in Fig. 7. $\alpha_D \ll 1$ also holds for this parameter range.

C. Quasinormal modes

From the ring-down phase seen in Fig. 4, it is possible to derive the complex frequencies of the fundamental quasinormal modes $\omega_{\rm QN}$. By comparing them with previous studies, we check the reliability of part of our results. In addition, the values of $\omega_{\rm QN}$ that have not been accurately computed for large values of D so far are derived from our numerical results.

The values of $\omega_{\rm QN}$ are evaluated in the following manner: The imaginary part $\mathrm{Im}(\omega_{\rm QN})$ is derived from the slope of the peaks of $\log\Phi(t)$ shown in Fig. 4. The real part is estimated by averaging the intervals of zeros of $\Phi(t)$, and consistency is checked by identifying the Fourier peak of $\Phi(t) \times \exp(-\mathrm{Im}(\omega_{\rm QN})t)$. For $D = 9$, 10, and 11, we found that two modes are mixed and searched two values of $\omega_{\rm QN}$ so that the numerical data of $\Phi(t)$ is well fitted. By comparing the results derived by using the several ranges of t, we estimate the error to be $\lesssim 1\%$ for $4 \le D \le 8$ and $\sim 5\%$ for $9 \le D \le 11$. We summarize the values of $\omega_{\rm QN}$ for $D =$ 4–11 in Table IV and compare the fitted data and $\Phi(t)$ for $D = 9$, 10, and 11 in Fig. 8.

The part of the derived results can be compared with previous ones. For $D = 4$, Leaver [33] gives very accurate values of $\omega_{\rm QN}$ (see [34] for a review). For the higher-dimensional Schwarzschild black holes, Konoplya [35] evaluated the values of $\omega_{\rm QN}$ for $l = 2$ and 3 using the

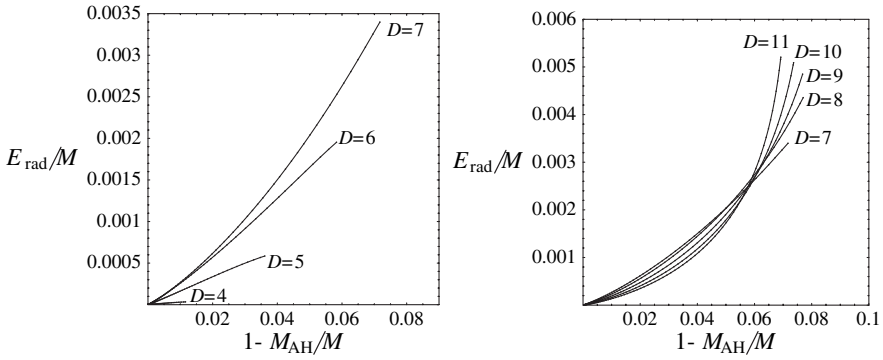

FIG. 7. The relation between $M - M_{\rm AH}$ and $E_{\rm rad}$ for $D = 4, \ldots, 7$ (left) and for $D = 7, \ldots, 11$ (right). The values of $E_{\rm rad}/(M - M_{\rm AH})$ are much smaller than unity. This is consistent with the area theorem.

TABLE IV. The fundamental quasinormal mode of the scalar gravitational perturbation in the Schwarzschild black hole for $l = 2$ and $4 \leq D \leq 11$. Results by our method, by Leaver's method, and by the WKB method are shown.

D	Our estimate	Leaver's method	WKB
4	$0.747 - 0.177i$	$0.7473 - 0.1779i$	$0.746 - 0.178i$
5	$0.947 - 0.256i$	$0.9477 - 0.2561i$	⋯
6	$1.139 - 0.305i$	⋯	$1.131 - 0.386i$
7	$1.339 - 0.400i$	⋯	⋯
8	$1.537 - 0.587i$	⋯	$[1.778 - 0.571i]$
9	$\begin{cases} 1.19 - 0.95i \\ 1.98 - 0.90i \end{cases}$	⋯	⋯
10	$\begin{cases} 1.25 - 0.94i \\ 2.47 - 0.99i \end{cases}$	⋯	$[2.513 - 0.744i]$
11	$\begin{cases} 1.20 - 0.98i \\ 2.91 - 1.11i \end{cases}$	⋯	⋯

WKB method and they were extended to $l \geq 4$ in [20]. The Leaver's method was applied to the scalar mode of the gravitational perturbation for $D = 5$ [36]. The values of $\omega_{\rm QN}$ derived with these methods are summarized in Table IV. In the cases $D = 4$ and 5, our results agree well with those in the previous studies. On the other hand, for $D = 6$, 8, and 10, our results disagree with the previous ones. As stated in [20,35], the WKB method is not expected to work well for $D = 8$ and 10 since the potential V_S has a negative peak. Our results indicate that the WKB method might not be good even for $D = 6$.

Our methods can be applied to arbitrary values of l. To estimate $\omega_{\rm QN}$, we evolved appropriate initial data for $l = 4$ and 6. For these cases, only one quasinormal frequency appears in the ring-down phase and the error of $\omega_{\rm QN}$ is $\lesssim 1\%$ for all values of D. Our results together with those in the previous studies are summarized in Tables V and VI. They agree well within the difference $\lesssim 1\%$. This implies that evolving appropriate initial data by the master equation is an effective method for computation of the complex frequencies of the fundamental quasinormal modes.

TABLE V. The same as Table IV but for $l = 4$.

D	Our estimate	Leaver's method	WKB
4	$1.618 - 0.188i$	$1.6184 - 0.1883i$	$1.618 - 0.188i$
5	$2.193 - 0.328i$	$2.1924 - 0.3293i$	⋯
6	$2.623 - 0.439i$	⋯	$2.622 - 0.438i$
7	$3.012 - 0.534i$	⋯	⋯
8	$3.389 - 0.631i$	⋯	$3.401 - 0.645i$
9	$3.779 - 0.734i$	⋯	⋯
10	$4.176 - 0.838i$	⋯	$4.223 - 0.841i$
11	$4.595 - 0.950i$	⋯	⋯

TABLE VI. The same as Table IV but for $l = 6$.

D	Our estimate	Leaver's method	WKB
4	$2.455 - 0.192i$	⋯	$2.424 - 0.191i$
5	$3.286 - 0.344i$	⋯	⋯
6	$3.913 - 0.470i$	⋯	$3.911 - 0.467i$
7	$4.610 - 0.574i$	⋯	⋯
8	$4.924 - 0.674i$	⋯	$4.923 - 0.675i$
9	$5.388 - 0.769i$	⋯	⋯
10	$5.834 - 0.859i$	⋯	$5.848 - 0.865i$
11	$6.292 - 0.955i$	⋯	⋯

V. SUMMARY

In this paper, we have studied gravitational waves emitted during head-on collision of two black holes in higher dimensions using the close-limit approximation. We evolved the Brill-Lindquist initial data perturbatively, using a gauge-invariant technique in a Schwarzschild black hole and calculated the waveform and radiated energy $E_{\rm rad}$. $E_{\rm rad}$ is given by the formula (25) and the values of $\hat{E}_2$ are summarized in Table II. At the critical separation for the presence of the common apparent horizon $z_0 = z_0^{(\rm crit)}$, our analysis of the first-order perturbation predicts that $E_{\rm rad}/M$ becomes larger with larger values of D. There is a possi-

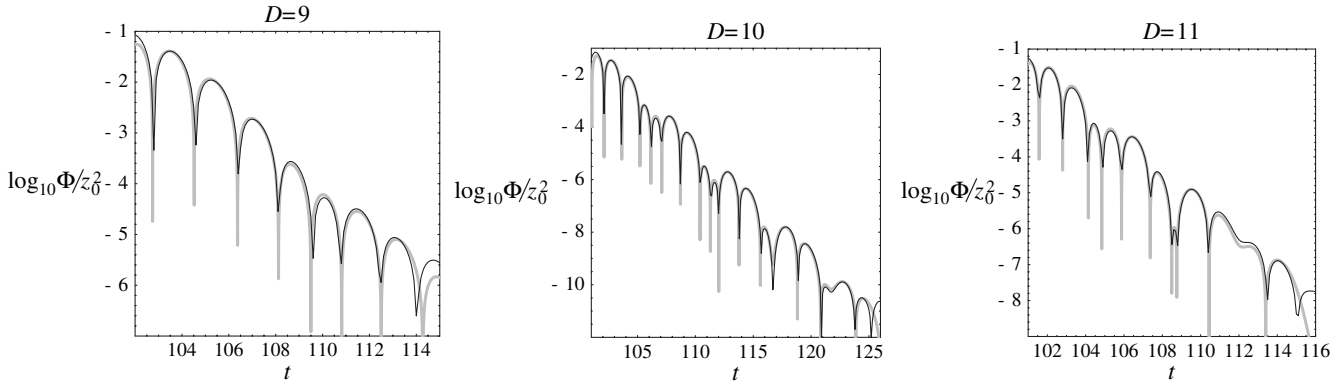

FIG. 8. The behavior of $\log_{10}\Phi(t)/z_0^2$ in the ringing phase (the black line) and the fitted data with two values of $\omega_{\rm QN}$ listed in Table IV (the gray line) for $D = 9$, 10, and 11.

bility that the higher-order correction is large for $z_0 = z_0^{(\mathrm{crit})}$ in the higher-dimensional cases and to clarify the higher-order effect is left as a remaining problem. We also evaluated the values of $\alpha_D = E_{\mathrm{rad}}/(M - M_{\mathrm{AH}})$ at $z_0 \ll 1$ and found that α_D $(5 \leq D \leq 11)$ is larger than α_4. These results indicate that more energy could be radiated away in higher-dimensional spacetimes than in the four-dimensional one during head-on collision with the approaching velocity much smaller than the speed of light.

It has also been illustrated that the fundamental quasinormal mode frequencies for the scalar-mode perturbation in the Schwarzschild black holes can be computed in our analysis. We derived the complex frequencies for various values of D, which have not been accurately computed so far.

As we mentioned in the Introduction, the close-limit analysis for head-on collision of the black holes performed in this paper is the first step toward more general studies of the black-hole collision in higher dimensions. As the next step, we plan to analyze the evolution of two initially moving black holes using the close-slow approximation. Both the head-on collisions and the grazing collisions should be studied. As the momentum of each black hole increases, dependence of the emissivity of gravitational waves on the value of D would be changed from the results in this paper. By observing such behaviors, we will be able to discuss the dependence of gravitational radiation in the collision process on the value of D in a different way from the previous studies.

ACKNOWLEDGMENTS

This work was supported by Grant-in-Aid for Scientific Research from Ministry of Education, Science, Sports, and Culture of Japan (No. 13135208, No. 14740155, No. 14102004, No. 17740136, and No. 17340075).

APPENDIX A: DETERMINING THE INITIAL MASTER VARIABLE

In this section, we explain how to match the initial master variable Φ to the initial data. We begin by briefly reviewing the gauge-invariant formulation of the perturbation in the Schwarzschild black-hole spacetime [29]. The background metric is given by

$$ds^2 = g_{ab}dy^a dy^b + r^2(y)\gamma_{ij}dz^i dz^j, \tag{A1}$$

where $g_{ab}dy^a dy^b = -fdt^2 + f^{-1}dr^2$ and $\gamma_{ij}dz^i dz^j$ denotes the metric on a unit sphere. The perturbed metric is written as

$$ds^2 = (g_{ab} + h_{ab})dy^a dy^b + (h_{ai} + h_{ia})dy^a dz^i + (r^2\gamma_{ij} + h_{ij})dz^i dz^j. \tag{A2}$$

The perturbation variables h_{ab}, h_{ai}, and h_{ij} can be separated into scalar, vector, and tensor modes. Each mode is further expanded into the modes of different angular quantum number $l = 0, 1, \ldots$ using the hyperspherical harmonics $\mathbb{S}$, which is the solution of the following equation:

$$(\hat{D}_i\hat{D}^i + k^2)\mathbb{S} = 0. \tag{A3}$$

Here $\hat{D}^i$ denotes the covariant derivative on the unit sphere and the definition of k^2 is given in Eq. (18). The variables of the scalar-mode perturbation are given by

$$h_{ab} = f_{ab}\mathbb{S}, \tag{A4}$$

$$h_{ai} = rf_a\mathbb{S}_i, \tag{A5}$$

$$h_{ij} = 2r^2(H_L\gamma_{ij}\mathbb{S} + H_T\mathbb{S}_{ij}), \tag{A6}$$

where

$$\mathbb{S}_i = -\frac{1}{k}\hat{D}_i\mathbb{S}, \tag{A7}$$

$$\mathbb{S}_{ij} = \frac{1}{k^2}\hat{D}_i\hat{D}_j\mathbb{S} + \frac{1}{n}\gamma_{ij}\mathbb{S}. \tag{A8}$$

In the axisymmetric case the metric of a unit sphere is written as

$$\gamma_{ij}dz^i dz^j = d\theta^2 + \sin^2\theta d\Omega_{n-1}^2, \tag{A9}$$

and then

$$\mathbb{S} = S_l^{[n]} \equiv K_l^{[n]}C_l^{[(n-1)/2]}(\cos\theta), \tag{A10}$$

$$K_l^{[n]} = \left[\frac{4\pi^{(n+1)/2}\Gamma(n+l-1)}{(n+2l-1)\Gamma(l+1)\Gamma((n-1)/2)\Gamma(n-1)}\right]^{-1/2}. \tag{A11}$$

$K_l^{[n]}$ is the normalization factor that is chosen so that

$$\int S_l^{[n]}S_{l'}^{[n]}d\Omega_n = \delta_{ll'} \tag{A12}$$

is satisfied. For the gauge transformation generated by the following vector fields,

$$\xi_a = T_a\mathbb{S}, \qquad \xi_i = rL\mathbb{S}_i, \tag{A13}$$

the gauge-invariant quantities of the perturbation are given by

$$F = H_L + (1/n)H_T + (1/r)D^a rX_a, \tag{A14}$$

$$F_{ab} = f_{ab} + D_aX_b + D_bX_a, \tag{A15}$$

where

$$X_a = \frac{r}{k}\left(f_a + \frac{r}{k}D_aH_T\right). \tag{A16}$$

The master variable Φ is related to the gauge-invariant quantities as follows:

$$X \equiv r^{n-2}(F_t^t - 2F) = r^{n/2-2}\left(-\frac{r^2}{f}\partial_t^2\Phi - \frac{P_X}{16H^2}\Phi + \frac{Q_X}{4H}r\partial_r\Phi\right), \quad \text{(A17)}$$

$$Y \equiv r^{n-2}(F_r^r - 2F) = r^{n/2-2}\left(\frac{r^2}{f}\partial_t^2\Phi - \frac{P_Y}{16H^2}\Phi + \frac{Q_Y}{4H}r\partial_r\Phi\right), \quad \text{(A18)}$$

$$Z \equiv r^{n-2}F_t^r = r^{n/2-1}\left(-\frac{P_Z}{4H}\partial_t\Phi + fr\partial_r\partial_t\Phi\right), \quad \text{(A19)}$$

where

$$P_X(r) = n^3(n+1)^3x^3 + 2n(n+1)[2(n^2+n+2)m - n(n-2)(n+1)]x^2 - 4n[(n-11)m + n(n+1)(n-3)]mx + 16m^3 + 8m^2n^2, \quad \text{(A20)}$$

$$Q_X(r) = n(n+1)^2x^2 + 2[(3n-1)m - n(n+1)]x - 4nm, \quad \text{(A21)}$$

$$P_Y(r) = n^3(n-1)(n+1)^2x^3 + 2n(n^2-1)[4m - n(n-2)\times(n+1)]x^2 + 4n(n-1)[3m + n(n+1)]mx, \quad \text{(A22)}$$

$$Q_Y(r) = n(n-1)(n+1)x^2 - 2(n-1)[m + n(n+1)]x, \quad \text{(A23)}$$

$$P_Z(r) = [-n^2(n+1)x + 2(n-2)m]y + n(n+1)x^2 + [2(2n-1)m + n(n+1)(n-2)]x - 2nm. \quad \text{(A24)}$$

Here, the definition of x is given in Eq. (18).

Now we turn our attention to the method for determining the initial master variable Φ from full nonlinear time-symmetric initial data. We denote f_{ab} and f_a as

$$f_{ab} = \begin{pmatrix} fH_0 & H_1 \\ H_1 & f^{-1}H_2 \end{pmatrix}, \qquad rf_a = (h_0, h_1). \quad \text{(A25)}$$

Because of the time symmetry of the initial condition,

$$\dot{H}_0 = \dot{H}_2 = \dot{h}_1 = \dot{H}_L = \dot{H}_T = 0, \quad \text{(A26)}$$

$$H_1 = h_0 = 0. \quad \text{(A27)}$$

By the comparison with Eqs. (12) and (14), we find

$$H_2 = 2H_L = \chi(r) \equiv \frac{1/(n-1)R^{n-1}}{1 + 1/4R^{n-1}}\left(\frac{z_0}{R}\right)^l (K_l^{[n]})^{-1}, \quad \text{(A28)}$$

$$h_1 = H_T = 0. \quad \text{(A29)}$$

Then the gauge-invariant quantity is found to be

$$F = H_L, \qquad F_r^t = 0, \quad \text{(A30)}$$

and thus

$$X + Y = -nr^{n-2}\chi(r), \quad \text{(A31)}$$

where we have used one of Einstein's equation $F_a^a = -2(n-2)F$. On the other hand, $X + Y$ is given in terms of Φ as follows:

$$X + Y = r^{n/2-2}\left(-\frac{P_X + P_Y}{16H^2}\Phi + \frac{Q_X + Q_Y}{4H}r\partial_r\Phi\right). \quad \text{(A32)}$$

Hence we find the following equation for the initial master variable Φ,

$$\frac{d\Phi}{dr_*} = \frac{f}{r(Q_X + Q_Y)}\left[\frac{P_X + P_Y}{4H}\Phi - 4nr^{n/2}H\chi(r)\right]. \quad \text{(A33)}$$

We also find $\dot{\Phi} = 0$ from the condition $Z = 0$.

Taking the limit $r_* \to -\infty$ of Eq. (A33), we find

$$\Phi = \frac{2 \cdot 4^{l/(n-1)}nz_0^l}{(n-1)(n+m)K_l^{[n]}}. \quad \text{(A34)}$$

This gives us the boundary condition at $r_* = -\infty$. We solve Eq. (A33) using the fourth-order Runge-Kutta method with the boundary condition (A34).

APPENDIX B: FORMULA OF RADIATED ENERGY

In this section, we sketch the derivation of Eq. (24). The similar calculation for the energy spectrum is found in Ref. [20].

In the region far from the source, outgoing waves are well approximated by the spherical ones in the transverse-traceless (TT). Then, the perturbation is written as

$$h_{ij}^{\rm TT} \simeq 2r^2H_T\mathbb{S}_{ij}, \quad \text{(B1)}$$

$$H_T \simeq \frac{A}{r^{n/2}}h(t-r). \quad \text{(B2)}$$

The radiated energy flux is given by

$$\frac{dE}{dSdt} = \frac{1}{32\pi G}\dot{h}_{ij}^{\rm TT}\dot{h}^{{\rm TT}ij} = \frac{1}{8\pi G}\dot{H}_T^2\mathbb{S}_{ij}\mathbb{S}^{ij}, \quad \text{(B3)}$$

which is the same form as in the four-dimensional case. Using the formula [20]

$$\mathbb{S}_{ij}\mathbb{S}^{ij} = \frac{1}{k^4}\hat{D}_i[\hat{D}_j\mathbb{S}\hat{D}^i\hat{D}^j\mathbb{S} + (k^2 - n + 1)\mathbb{S}D^i\mathbb{S}] + \frac{(k^2-n)(n-1)}{k^2n}\mathbb{S}^2, \quad \text{(B4)}$$

we find

$$\frac{dE}{dt} = r^n\frac{\dot{H}_T^2}{8\pi G}\frac{(n-1)(k^2-n)}{nk^2}. \quad \text{(B5)}$$

Next we rewrite the formula (B5) in terms of the master variable Φ. In a region far from the source, the gauge-invariant quantities become

$$F = \frac{1}{n} H_T + \frac{f}{r} X_r, \qquad F_{ab} = D_a X_b + D_b X_a, \tag{B6}$$

$$X_a = \frac{r^2}{k^2} \partial_a H_T. \tag{B7}$$

If we calculate F, F_t^t, F_r^r, and F_t^r keeping only the leading order $O(r^{2-n/2})$ and the subleading order $O(r^{1-n/2})$, we find

$$Y + Z = n \frac{r^{n-1}}{k^2} \dot{H}_T, \tag{B8}$$

where Eq. (B2) was also used. On the other hand, calculating $Y + Z$ in terms of Φ and using the fact that $\ddot{\Phi} = -\partial_r \dot{\Phi}$ holds for the outgoing wave, we obtain

$$\dot{H}_T = \frac{k^2}{2} r^{-n/2} \dot{\Phi}. \tag{B9}$$

Substituting this equation into Eq. (B5), we find

$$E_{\rm rad} = \sum_l \frac{k^2 (n-1)(k^2-n)}{32\pi n G} \int \dot{\Phi}^2 dt. \tag{B10}$$

This formula is equivalent to Eq. (24) in the unit $r_h(M) = 1$.

Using Eqs. (B3), (B9), and (B10), we find

$$\frac{1}{E} \frac{dE}{d\Omega_n} = \frac{1}{k^2 (k^2-n)(n-1)^2} (n \mathbb{S}_{,\theta\theta} + k^2 \mathbb{S})^2. \tag{B11}$$

In the case of $l = 2$, it becomes

$$\frac{1}{E} \frac{dE}{d\Omega_n} = \frac{2\pi^{-(n+1)/2} \Gamma((n+5)/2)}{n(n+2)} \sin^4\theta, \tag{B12}$$

which reduces to Eq. (26) using $d\Omega_n = \Omega_{n-1} \sin^{n-1}\theta d\theta$.

[1] N. Arkani-Hamed, S. Dimopoulos, and G. R. Dvali, Phys. Lett. B **429**, 263 (1998); I. Antoniadis, N. Arkani-Hamed, S. Dimopoulos, and G. R. Dvali, *ibid.* **436**, 257 (1998).

[2] L. Randall and R. Sundrum, Phys. Rev. Lett. **83**, 3370 (1999).

[3] T. Banks and W. Fischler, hep-th/9906038; S. B. Giddings and S. Thomas, Phys. Rev. D **65**, 056010 (2002); S. Dimopoulos and G. Landsberg, Phys. Rev. Lett. **87**, 161602 (2001).

[4] G. Landsberg, hep-ph/0211043; M. Cavaglia, Int. J. Mod. Phys. A **18**, 1843 (2003); P. Kanti, Int. J. Mod. Phys. A **19**, 4899 (2004); S. Hossenfelder, hep-ph/0412265.

[5] P. Kanti and J. March-Russell, Phys. Rev. D **66**, 024023 (2002); P. Kanti and J. March-Russell, Phys. Rev. D **67**, 104019 (2003); D. Ida, K. Y. Oda, and S. C. Park, Phys. Rev. D **67**, 064025 (2003); **69**, 049901(E) (2004); D. Ida, K. Y. Oda, and S. C. Park, Phys. Rev. D **71**, 124039 (2005); C. M. Harris and P. Kanti, hep-th/0503010.

[6] S. Dimopoulos and R. Emparan, Phys. Lett. B **526**, 393 (2002); E. J. Ahn, M. Cavaglia, and A. V. Olinto, Phys. Lett. B **551**, 1 (2003); M. Cavaglia, S. Das, and R. Maartens, Classical Quantum Gravity **20**, L205 (2003); M. Cavaglia and S. Das, Classical Quantum Gravity **21**, 4511 (2004).

[7] R. Emparan, G. T. Horowitz, and R. C. Myers, Phys. Rev. Lett. **85**, 499 (2000); V. Frolov and D. Stojkovic, Phys. Rev. D **67**, 084004 (2003); **68**, 064011 (2003); M. Cavaglia, Phys. Lett. B **569**, 7 (2003); D. Stojkovic, Phys. Rev. Lett. **94**, 011603 (2005).

[8] S. B. Giddings and V. S. Rychkov, Phys. Rev. D **70**, 104026 (2004).

[9] V. S. Rychkov, Phys. Rev. D **70**, 044003 (2004); Int. J. Mod. Phys. A **20**, 2398 (2005); hep-th/0410295.

[10] P. C. Aichelburg and R. U. Sexl, Gen. Relativ. Gravit. **2**, 303 (1971).

[11] D. M. Eardley and S. B. Giddings, Phys. Rev. D **66**, 044011 (2002).

[12] H. Yoshino and Y. Nambu, Phys. Rev. D **67**, 024009 (2003).

[13] H. Yoshino and V. S. Rychkov, Phys. Rev. D **71**, 104028 (2005).

[14] R. C. Myers and M. J. Perry, Ann. Phys. (N.Y.) **172**, 304 (1986).

[15] V. Cardoso, E. Berti, and M. Cavaglia, Classical Quantum Gravity **22**, L61 (2005).

[16] P. D. D'Eath and P. N. Payne, Phys. Rev. D **46**, 658 (1992); **46**, 675 (1992); **46**, 694 (1992).

[17] P. D. D'Eath, *Black Holes: Gravitational Interactions* (Oxford Science Publications, Oxford, 1996).

[18] V. Cardoso, O. J. C. Dias, and J. P. S. Lemos, Phys. Rev. D **67**, 064026 (2003).

[19] V. Cardoso and J. P. S. Lemos, Phys. Lett. B **538**, 1 (2002).

[20] E. Berti, M. Cavaglia, and L. Gualtieri, Phys. Rev. D **69**, 124011 (2004).

[21] V. Cardoso and J. P. S. Lemos, Gen. Relativ. Gravit. **35**, 327 (2003); Phys. Rev. D **67**, 084005 (2003); V. Cardoso, J. P. S. Lemos, and S. Yoshida, Phys. Rev. D **68**, 084011 (2003).

[22] L. Smarr, A. Cadez, B. S. DeWitt, and K. Eppley, Phys. Rev. D **14**, 2443 (1976); L. Smarr, in *Sources of Gravitational Radiation*, edited by L. Smarr (Cambridge University Press, Cambridge, England, 1979), p. 245; P. Anninos, D. Hobill, E. Seidel, L. Smarr, and W. M. Suen, Phys. Rev. Lett. **71**, 2851 (1993); Phys. Rev. D **52**, 2044

(1995); J. Baker, A. Abrahams, P. Anninos, S. Brandt, R. Price, J. Pullin, and E. Seidel, Phys. Rev. D **55**, 829 (1997); P. Anninos, S. Brandt, and P. Walker, Phys. Rev. D **57**, 6158 (1998); B. Brugmann, Int. J. Mod. Phys. D **8**, 85 (1999); S. Brandt *et al.*, Phys. Rev. Lett. **85**, 5496 (2000); M. Alcubierre, W. Benger, B. Brugmann, G. Lanfermann, L. Nerger, E. Seidel, and R. Takahashi, Phys. Rev. Lett. **87**, 271103 (2001); J. Baker, B. Brugmann, M. Campanelli, C. O. Lousto, and R. Takahashi, Phys. Rev. Lett. **87**, 121103 (2001); J. Baker, M. Campanelli, and C. O. Lousto, Phys. Rev. D **65**, 044001 (2002); J. Baker, M. Campanelli, C. O. Lousto, and R. Takahashi, Phys. Rev. D **65**, 124012 (2002); M. Alcubierre, B. Brugmann, P. Diener, M. Koppitz, D. Pollney, E. Seidel, and R. Takahashi, Phys. Rev. D **67**, 084023 (2003); B. Bruegmann, W. Tichy, and N. Jansen, Phys. Rev. Lett. **92**, 211101 (2004); J. Baker, M. Campanelli, C. O. Lousto, and R. Takahashi, Phys. Rev. D **69**, 027505 (2004); B. Imbiriba *et al.*, Phys. Rev. D **70**, 124025 (2004); M. Alcubierre *et al.*, Phys. Rev. D **72**, 044004 (2005); M. Campanelli, Classical Quantum Gravity **22**, S387 (2005); U. Sperhake, B. Kelly, P. Laguna, K. L. Smith, and E. Schnetter, Phys. Rev. D **71**, 124042 (2005); Y. Zlochower, J. G. Baker, M. Campanelli, and C. O. Lousto, Phys. Rev. D **72**, 024021 (2005); F. Pretorius, Phys. Rev. Lett. **95**, 121101 (2005).

[23] R. H. Price and J. Pullin, Phys. Rev. Lett. **72**, 3297 (1994).

[24] A. M. Abrahams and R. H. Price, Phys. Rev. D **53**, 1972 (1996).

[25] Z. Andrade and R. H. Price, Phys. Rev. D **56**, 6336 (1997).

[26] A. M. Abrahams and G. B. Cook, Phys. Rev. D **50**, R2364 (1994); G. Khanna *et al.*, Phys. Rev. Lett. **83**, 3581 (1999); G. Khanna, R. Gleiser, R. Price, and J. Pullin, New J. Phys. **2**, 3 (2000).

[27] W. Krivan and R. H. Price, Phys. Rev. Lett. **82**, 1358 (1999); C. O. Lousto, Phys. Rev. D **63**, 047504 (2001); M. Campanelli, R. Gomez, S. Husa, J. Winicour, and Y. Zlochower, Phys. Rev. D **63**, 124013 (2001); G. Khanna, Phys. Rev. D **63**, 124007 (2001); J. Baker, M. Campanelli, and C. O. Lousto, Phys. Rev. D **65**, 044001 (2002); S. Husa, Y. Zlochower, R. Gomez, and J. Winicour, Phys. Rev. D **65**, 084034 (2002); R. J. Gleiser and A. E. Dominguez, Phys. Rev. D **65**, 064018 (2002); O. Sarbach, M. Tiglio, and J. Pullin, Phys. Rev. D **65**, 064026 (2002); J. Baker, M. Campanelli, C. O. Lousto, and R. Takahashi, Phys. Rev. D **65**, 124012 (2002); G. Khanna, Phys. Rev. D **66**, 064004 (2002).

[28] D. R. Brill and R. W. Lindquist, Phys. Rev. **131**, 471 (1963).

[29] H. Kodama and A. Ishibashi, Prog. Theor. Phys. **110**, 701 (2003).

[30] H. Yoshino and Y. Nambu, Phys. Rev. D **70**, 084036 (2004).

[31] S. W. Hawking, J. Math. Phys. (N.Y.) **9**, 598 (1968).

[32] V. Cardoso, S. Yoshida, O. J. C. Dias, and J. P. S. Lemos, Phys. Rev. D **68**, 061503(R) (2003).

[33] E. W. Leaver, Proc. R. Soc. A **402**, 285 (1985).

[34] K. D. Kokkotas and B. G. Schmidt, Living Rev. Relativity **2**, 2 (1999).

[35] R. A. Konoplya, Phys. Rev. D **68**, 024018 (2003); **68**, 124017 (2003).

[36] V. Cardoso, J. P. S. Lemos, and S. Yoshida, J. High Energy Phys. 12 (2003) 041.